

CARESS Working Paper #02-02

“CHAOS THEORY AND ITS APPLICATION”

By

Haim H. Bau and Yochanan Shachmurove



UNIVERSITY of PENNSYLVANIA

Center for Analytic Research

in Economics and the Social Sciences

McNEIL BUILDING, 3718 LOCUST WALK

PHILADELPHIA, PA 19104-6297

Chaos Theory and Its Application

Haim H. Bau

Department of Mechanical Engineering and Applied Mechanics,
University of Pennsylvania, Philadelphia, PA 19104-6315, USA

E-mail: bau@eniac.seas.upenn.edu

And

Yochanan Shachmurove

Departments of Economics, The City College of The City University
of New York and The University of Pennsylvania

E-mail: Yochanan@econ.sas.upenn.edu

Abstract

One consequence of dynamic system theory is that relatively simple systems, which can be described by a few non-linear equations, can exhibit very complicated, stochastic-like behavior. Such models simulate processes inexpensively. They reveal insights into the underlying mechanisms while devising strategies to control these processes.

Chaotic systems are sensitive to initial conditions. Since these conditions are not precisely known and are subject to perturbations, long-term predictions of the behavior of these systems are impossible. Thus, the availability of large computational resources will **not** enable one to generate long-term predictions for systems ranging from weather to economic forecasts.

Key Words: Chaos Theory, Deterministic Systems, Stochastic Behavior, Lyapunov Exponent, Non-linear Models, Lorenz Loop, Random-looking Oscillations, Poinaré, Magneto Hydrodynamic Stirrer, Phase Space, Embedding Theorem, Power Spectrum, Information Dimension.

Introduction

The last few decades have seen an increased emphasis on mathematical modeling. One class of models consists of evolution equations: the description of the time-dependence or the dynamics of various processes through mathematical statements written either as differential equations for continuous processes or difference equations for discrete processes. Such models have been of great utility in the physical and natural sciences, engineering, and economics. Just a few examples of such models are the oscillations of a pendulum, the weather system, streams in the ocean, the spread of diseases, physiological rhythms, and population dynamics. Broadly speaking, mathematical models can be classified as either deterministic or stochastic. Since our intention is to avoid technical jargon and to make the presentation simple, we define a deterministic process as a process that when repeated exactly in the same way will yield exactly the same outcome. In contrast, stochastic processes will yield different outcomes when repeated. Here, we will focus solely on deterministic processes.

One may be tempted to conclude that deterministic systems exhibit only regular behavior and that once a deterministic model is available, one should be able to predict the system's future behavior. In other words, if we know the system's current state, we should be able to tell the system's future states at all

times. Although many systems do exhibit regular and predictive behavior, there are many others that do not. In fact, there are many deterministic systems that exhibit irregular, random-like behavior. Such systems are referred to as chaotic. We reemphasize that, in the context of this paper, we define chaotic systems as deterministic systems that exhibit complex behavior.

One of the characteristics of chaotic systems is high sensitivity to initial conditions. When a system exhibits high sensitivity to initial conditions, even when we have an accurate model for that system, we cannot predict its future behavior. Any small inaccuracy in the initial data, such as may result from measurement errors, will amplify rapidly and will render any long-term prediction useless. The possibility of initial errors growing rapidly is common to all unbounded systems (linear systems included) that exhibit exponential growth. Less widely known is the fact that such sensitivity to initial conditions is exhibited by many nonlinear, bounded systems.

The prominent French mathematician, dynamist, and astronomer, Henri Poincaré is credited to be the first to realize that "... it may happen that small differences in the initial conditions produce very great ones in the final phenomena. A small error in the former will produce an enormous error in the latter. Prediction becomes impossible, and we have the fortuitous phenomenon" (Poincaré, 1913). A detailed depiction of the complex behavior exhibited by chaotic systems was delayed

until the appearance of computers that allowed one to investigate numerically the behavior of continuous models over relatively long time intervals and discrete models over many iterations. In 1963, while he was studying various simplified models for the weather system, the meteorologist E. N. Lorenz observed that a deceptively simple-looking system of three coupled, nonlinear differential equations exhibits complex (chaotic) behavior. Although the scientific community recognized that deterministic systems may exhibit random-like, turbulent behavior, the prevailing dogma had been that such behavior would be exhibited only by systems with very many degrees of freedom. Lorenz's work demonstrated that a system with a relatively small number of degrees of freedom (as few as three) may also exhibit chaotic behavior. Although deterministic systems may exhibit random-like behavior that resembles the behavior of stochastic (random) systems, such irregularity results from the system's intrinsic dynamics, and not random influences.

The fact that certain systems may exhibit chaotic, unpredictable behavior has very important practical and philosophical implications. The lack of predictability of chaotic systems cannot be cured by increases in computer and computational power. No matter how large a computer one would acquire, the chaotic system will still remain unpredictable over the long-term. The realization that low-dimension systems may exhibit chaotic, complex behavior suggests that some complex

phenomena that appear to be random at first sight may be describable by relatively low-dimensional mathematical models. One of the targets of such investigations (apparently with little or no success) has been the stock market. Of course, there is no assurance that the market fluctuations result from chaotic dynamics. Although the chaotic dynamics defy long-term predictions, short-term predictions with error estimates can still be made. Furthermore, with an observer that observes some of the system's states, it is possible to devise a state estimator capable of updating and modifying predictions. Finally, many chaotic systems are controllable. One can suppress their chaotic behavior altogether or induce them to behave periodically with various periods. This leads to the opportunity of extracting many types of behavior from a single system with minimal intervention. Moreover, occasionally it may be beneficial to induce chaos under conditions when it would normally not occur. For example, chaotic behavior is often associated with high levels of stirring and mixing which is desirable for homogenization as well as chemical and biological reactions.

Chaos is a ubiquitous phenomenon that crosses disciplinary lines. The topic has attracted a great amount of attention in the last two decades. There are a great number of excellent and not so excellent books focused on this topic as well as a number of professional journals. A month will hardly go by without a new book or compendium devoted to chaos theory appearing in

print. There are journals devoted to chaos theory, and hundreds of research papers on this topic appear annually. The literature ranges from highly readable non-technical books such as Gleick's (1987) bestseller, and Peitgen and Richter's (1986) coffee table images, to the engineering/physics literature and highly mathematical manuscripts. This paper targets a non technical audience seeking to obtain somewhat greater exposure than that offered by the non technical literature, albeit without inordinate immersion in technical details. To facilitate this quest, we shall therefore introduce the topic through the description of two chaotic toys. Although these toys were chosen from the authors' areas of expertise, the phenomena described and its implications are generic and cross disciplinary lines. The first toy - the Lorenz loop - exhibits temporal chaos while the second toy - the electro-magneto hydrodynamic stirrer - exhibits spatial chaos.

The Lorenz Loop

The first "toy" is a thermal convection loop. We refer it as the Lorenz loop because it can be approximately modeled by the Lorenz equations. In other words, this set-up is an experimental analog of the Lorenz model. Imagine a pipe bent into a torus (doughnut-shape) and standing in the vertical plane. See Figure 1 for the schematic depiction of the apparatus.

INSERT FIGURE 1

The tube is filled with liquid (i.e., water) The lower half of the apparatus is heated while the upper half is cooled. The heating and cooling conditions are symmetric with respect to the loop's axis that is parallel to the gravity vector. As a result of the heating, the liquid in the lower half of the apparatus expands, its density decreases, and it tends to rise. When the heating rate exceeds a certain critical value, irregular flow is observed in the loop. The flow rate oscillates irregularly in time with occasional reversals of the direction of the flow. We denote the flow rate as X , the temperature difference between positions 3 and 9 o'clock across the loop as Y , and the temperature difference between positions 6 and 12 o'clock as Z . These three variables, all of which are functions of time, are sufficient to describe the major features of the flow dynamics in the loop. The solid line in Figure 2 depicts the computed flow rate (X) as a function of time when the heating rate is held constant at some value.

INSERT FIGURE 2

The documentation of a signal as a function of time as we did in Figure 2 is referred to as a *time-series*. Witness the irregular, random-looking oscillations, i.e., periodic motion about an equilibrium position. Positive and negative values of X correspond, respectively, to motion in the counterclockwise and

clockwise directions. Let us denote, respectively, the positive and negative peaks with P and N and document the succession of peaks and valleys as $N^2PN^2PN^2PN^2P^8\dots$. In other words, the above sequence implies two negative peaks followed by a positive one, etc. This sequence is reminiscent of the random sequence that one would obtain when tossing a coin and counting the sequence of heads (P) and tails (N). Yet, the signal described in Figure 2 is fully deterministic, and there is nothing random about it. Similar behavior to that depicted in Figure 2 has been observed in experiments. Furthermore, behaviors like the one depicted in Figure 2 prevail in many systems. For example, one can think of X, Y, and Z as representing the fluctuations around a mean value of the populations of three interacting species.

In Figure 2, we depicted also a second time-series (dashed line). This second time series was generated by the same mathematical model as the first one, albeit with slightly different initial conditions. Although the two signals initially stay close to each other, eventually the time series diverge and exhibit significantly different behaviors. This is a result of the high sensitivity to initial conditions. The divergence does not continue indefinitely as the system is bounded, and X never exceeds certain values. Only non-linear systems can exhibit bounded behavior with high sensitivity to initial conditions or disturbances. Chaotic behavior can be exhibited only by nonlinear systems.

The time series depicted in Figure 2 seems to lack structure. Indeed, traditional methods of analyzing time series such as presenting the data in the frequency domain (Fourier transform and power spectrum) reveal a broadband signal lacking any dominating frequencies. Nevertheless, the signal depicted in this Figure has fair amount of order to it. To unravel this order, we will depict the signal in a space spanned by the coordinates X , Y , and Z (the *phase space*). The state of the system at any instant in time is specified by a point (X, Y, Z) in phase space. The time evolution of the system is depicted by a curve (*trajectory*) in phase space. It is useful to think of the system's state as a particle roaming around in space.

INSERT FIGURE 3

Figure 3 depicts the phase portrait of the Lorenz loop. Witness that the phase portrait of the system has a fair amount of structure to it. Indeed, there is an amazing tendency for self-organization. No matter what the system's initial conditions are, eventually, the trajectories will follow a similar pattern. The trajectories in Figure 3 appear to lie on a twisted surface. The feature to which the trajectories are attracted is called an *attractor*. Since the structure of the attractor depicted in Figure 3 is complicated, it is referred to as a *strange attractor*. Attractors are present only in

dissipative system, i.e., systems that do not preserve "potential energy" but dissipate energy such as when friction is present. In our example, the phase space is three-dimensional, and the attractor occupies zero volume in the three-dimensional phase space; so its dimension must be smaller than 3. The sheet occupied by the attractor has a sort of "onion" feature to it, as it contains numerous layers. Hence the attractor must have a dimension larger than 2 (2 is the dimension of a surface). This suggests generalizing the concept of dimension to include fractional dimensions -known as *fractal dimensions*. In our case, the attractor's fractal dimension is approximately 2.07.

The phase space portrait is very useful for obtaining qualitative information on the nature of the solutions of differential equations. For example, closed trajectories indicate periodic behavior. Barring pathological behavior (which usually does not occur in physical systems), evolution equations have a unique solution. In other words, once the initial conditions have been specified, the system will trace a unique trajectory in phase space. This implies that trajectories cannot cross. In two-dimensional space, trajectories cannot intersect and the most complicated behavior that an autonomous, continuous, bounded system can exhibit is periodic oscillations. To exhibit chaotic behavior, continuous autonomous systems must be at least three-dimensional (three degrees of freedom). Such a restriction does not apply to discrete systems. Discrete systems lack

continuous trajectories; and points in phase space can jump around. In fact, even one-dimensional, nonlinear discrete systems may exhibit chaotic behavior. One celebrated example of a one-dimensional, discrete chaotic system is the logistic equation.

The phase space portrait in Figure 3 was constructed using the mathematical model to compute the trajectories. The attractor can also be reconstructed based on a time series. One can carry out measurements and obtain a time series for a single variable, say X , as a function of time (t). One then constructs a "comb" with P teeth placed at distances τ apart from each other. Guidelines are available for the range of desirable τ values. One then slides the comb along the time axis and extracts the points at which the comb intersects the curve traced by the time series (i.e., Figure 2) to obtain the variables X_1, X_2, \dots, X_P . These variables are considered to be the coordinates of a point in the P -dimensional phase space. The collection of all these points in phase space provides a description of the attractor. This technique is especially useful when the mathematical model is not known, and one analyzes empirical data and when the mathematical model has very many degrees of freedom and one wishes to determine the feasibility of describing the dynamics with a low dimension model. When the dimensionality of the dynamic system is not *a priori* known, the practice is to start with a relatively small value of P , for example $P=3$, reconstruct

the attractor, and calculate its dimension (D_A). Then increase P gradually, and compute D_A as a function of P . Typically, D_A will initially increase as P increases. When the time series is generated by a chaotic system, eventually, once P is sufficiently large, D_A will saturate, achieve a constant value, and will no longer vary with further increases in P . The value of P beyond which the fractal dimension no longer depends on P is the estimate of the systems' number of significant degrees of freedom. The above procedure allows us to test whether a signal is generated by a chaotic or a stochastic system. In stochastic systems, there is no attractor and D_A will keep increasing indefinitely as P increases. Of course, such a procedure is practical only for relatively low-dimension systems. Using this technique, one can reconstruct different attractors. All of these attractors, however, are related through smooth transformations. As funky as this technique may sound, it has rigorous foundations. Its practical applications may not always be straightforward, if only, because measured signals may be contaminated with noise that must be filtered out.

Another way of analyzing the phase space portrait is by documenting the penetration points of trajectories through a designated surface in phase space.

INSERT FIGURE 4

Figure 4 depicts the penetration points through the plane $Z=Z_0=\text{constant}$. Such portraits are known as *Poincaré sections*.

At first glance, the Poincaré section appears to consist of line segments, which would imply that the attractor is confined to a two-dimensional sheet. In fact, when we zoom on the line, we discover that it consists of a very large number of closely packed sheets. The structure appears to be *self-similar* in the sense that each additional magnification reveals a structure similar to the one we saw in the previous magnification. The n -th penetration in the Poincaré section relates to the previous one through a two-dimensional map of the form $\{x_{n-1}, y_{n-1}\} \rightarrow \{x_n, y_n\}$. In effect, the Poincaré section converts the continuous model to a discrete one, allowing us to make a connection between continuous and discrete models. Often when a system is forced periodically in time, the Poincaré section will consist of *stroboscopic images* (images taken once every period) of the system's state. This is explained in greater details in the next section.

Although chaotic systems defy long-term predictions, short terms predictions are possible. One can estimate the rate of divergence of the trajectories. This rate of divergence is known as the *Lyapunov exponent* and one can estimate the prediction's error as a function of the error in estimating the initial state and the estimation time interval. Moreover, with the aid of an observer, the state of the chaotic system can be estimated in the presence of disturbances and uncertainty in initial conditions. The observer continuously monitors one or more of the state

variables or some other state-dependent measurant. The system's behavior is estimated with the aid of its mathematical model plus an extra term (filter) that is a function of the difference between the actually measured and the predicted values.

Finally, chaotic systems are controllable. With the use of a feedback controller, one can suppress the chaotic behavior completely, and obtain time-independent behavior (i.e., when one depicts X as a function of time, one would obtain a nearly straight horizontal line). See Singer et al., (1991). In fact, the chaotic attractor contains numerous non-stable, periodic orbits of various periodicities. It is possible to use a controller to stabilize any desired period. Thus, one can obtain very many types of behaviors from a single chaotic system. For example, researchers have determined that the irregular beatings of the atrial chambers of the heart are chaotic. Through the application of electrical stimuli in a feedback mode, they were able to control the cardiac arrhythmia in a rabbit. Similarly, apparently chaotic electrical patterns characteristic of epileptic behavior in the rat brain tissue (cf. paper by Gur, Contreras, Gur) have been controlled with the aid of a feedback controller.

Of equal interest is the problem of using a controller to induce chaos in systems that are naturally well behaved (laminar). Chaotic systems usually exhibit efficient stirring. Efficient stirring is desirable in chemical and biological

reactions. We shall explore the use of chaos to induce steering in the next section and this will give us the opportunity also to encounter spatial chaos.

The Magneto Hydrodynamic Stirrer

The magneto-hydrodynamic stirrer consists of a circular cavity with an electrode C deposited around its periphery. Two additional electrodes A and B are deposited eccentrically inside the cavity on the cavity's bottom. See Figure 5.

Insert Figure 5

The cavity is positioned in a uniform magnetic field that is parallel to the cavity's axis, and it is filled with a weak electrolyte solution such as saline solution. When a potential difference is applied across electrodes A-C, where A is positive and C is negative, electric current will flow in the solution between the two electrodes. The interaction between the current and the magnetic field results in Lorenz forces that, in turn, induce, say, counter clockwise flow circulation in the cavity. The motion can be traced by seeding the liquid with small particles. The trajectories of some of such particles are depicted in Figure 6. We refer to this flow pattern as pattern A. When we apply a potential difference across electrodes B-C, where B is negative and C is positive, now a clockwise circulation will be induced around electrode B. We refer to this

flow pattern as pattern B. We operate the device by alternately engaging electrodes A-C and C-B with a period T . Each electrode pair is engaged for a time interval equal to half the period.

Insert Figure 6

Figure 7 depicts stroboscopic images (Poincaré sections) of the tracer's location at the end of each period. When the alterations are at high frequency (Figure 7a), the tracer tracks a trajectory that is nearly a superposition of patterns A and B. At moderate values of T (Figure 7b), one observes the appearance of irregular chaotic islands. When T is further increased, the chaos spreads into the entire cavity (Figure 7c).

Insert Figure 7

The chaotic behavior is characterized by the irregular spread of points. Witness that the chaotic behavior is induced by alternating two regular flow patterns of the types depicted in Figure 6. This phenomenon is known as Lagrangian chaos. In contrast to our first example where the chaotic behavior was temporal; here the chaotic behavior is spatial. The other features of chaos such as high sensitivity to initial conditions are also present here. In other words, if we place two tracer particles next to each other, their trajectories will markedly diverge as time goes by.

To see additional features of the chaotic advection, we will trace the evolution of a trace of dye introduced into the fluid when the period T is relatively large (same period as in Figure 7). In Figure 8a, we place a black blob inside the cavity. Figures 8b, 8c, 8d, 8e, and 8f depict, respectively, the same material blob after 10, 20, 30, 40, and 50 time periods. Witness that the flow stretches material lines (Figure 8b)

INSERT FIGURE 8

Since the flow is bounded (confined to the cavity), the stretching cannot continue indefinitely and the material lines are forced to fold. The process increases the interface between the two materials and this is why chaotic flows provide for efficient stirring. The process depicted in Figure 8 is governed by kinematics alone, and it does not include any molecular diffusion. This process of continuous stretching and folding is characteristic of chaotic dissipative systems and it is also present in the Lorenz attractor.

Beyond Physics and Engineering

So far, we have discussed concrete examples taken from the world of engineering and physics. Earlier in the paper, we hinted about possible extensions to biological and social systems. Indeed, biology, finance, economics, and social

phenomena yield complex time and spatial evolutions that often appear to be stochastic and unpredictable. It is natural to wonder whether such phenomena can be attributed to endogenous (intrinsic) mechanisms (described with deterministic models) or exogenous influences (described by stochastic noise). Although in these systems, the driving forces are quite different (and often more difficult to discern) than in physical systems, the patterns of behavior are often phenomenologically similar to the ones displayed by deterministic chaotic systems. Indeed, Dynamic System Theory crosses disciplinary lines.

For many years, biologists and population dynamists have been aware of population fluctuations. As early as 1926, Volterra proposed a simple predator-prey model to explain the annual fluctuations of certain fish catches in the Adriatic. Perhaps the simplest model of population dynamics is the one that describes the evolution of a single species. Let X_n denote the number of members of a certain species at generation (n). With appropriate normalization ($0 < X_0 < 1$, $1 < \lambda < 4$), the number of individuals in generation ($n+1$), X_{n+1} , is modeled as $X_{n+1} = \lambda X_n (1 - X_n)$. In the above, the first term represents the growth rate. When X_n is small, the growth rate is nearly a linear function of X_n . When X_n is relatively large, limited resources and crowding check the size of the population. The above equation is known as the *discrete logistic map*. It is easy to iterate this equation on a hand-held calculator and observe

the various patterns that evolve for various values of λ . Clearly, the size of the population is bounded ($0 \leq X_n \leq 1$). As λ increases, the population's evolution patterns vary from time-independent to time-periodic, with various periodicities to chaotic (irregular) behavior; that is to say, with high sensitivity to initial conditions. The logistic model can be readily enriched (and made more complicated) by including interactions between two or more competing species, as in the predator-prey model. It is perhaps not surprising that models of population dynamics have been used with various degrees of success to study, among other things, the cause and spread of epidemic outbreaks and the effectiveness of vaccinations.

Analysis of Economic Data - An example of An Application

Models similar to the ones used in population dynamics have been utilized also to simulate various economic phenomena such as the relationships between prices and commodity quantities, capital growth, and business cycles. Business cycles, for example, are often likened in their unpredictability to turbulent flow. Nonlinear mathematical models can duplicate complex behaviors qualitatively, in ways similar to those observed in economic systems. This, however, does not necessarily imply that economic systems are chaotic, in the sense of deterministic chaos. For example, Forsyth (1994) claims that the behavior of the international financial market in the 1990s is remarkably

similar to the behavior of local markets in the 1890s, suggesting a possible deterministic pattern.

Recognizing the existence of deterministic chaos in economic data is important from both theoretical and practical points of view. From the theoretical point of view, knowing that a system is chaotic may assist in constructing mathematical models, which would provide a deeper understanding of the underlying dynamics. From the practical point of view, such a model may facilitate process control and, in some cases, short-term predictions. The high sensitivity of chaotic systems to small perturbations makes long-term predictions impossible. Nevertheless, in some cases, short-term predictions within estimable error margins are not beyond the realm of possibility.

Weak-form market efficiency has long been the subject of empirical scrutiny. The weak-form market efficiency hypothesis states that future securities prices cannot be predicted from current and past price and market information. This hypothesis suggests that investors cannot reliably earn abnormal returns merely by looking at universally available information. However, the weak-form market efficiency should not be confused with the "random walk" theory of market efficiency (Fama, 1970). Random walk theories maintain that stock returns are identically and independently distributed, and that the sole indicator of future prices is the current price. Unlike random walk theories, weak-form efficiency does not claim that stock returns are stochastic

given all unobserved information. It does claim that stock prices are stochastic, under only past price and market data information.

The most basic test of the weak-form efficiency hypothesis is autocorrelation. This test fits the time-series of excess returns to a linear regression model. The excess return is equal to the actual minus the expected return, which is determined from models such as the Capital Asset Pricing Model (Fama and MacBeth, 1973)

Autocorrelation studies strongly support the weak-form market efficiency theory. Cootner (1974) studies the relationship between forty-five U.S. stock returns, over one and fourteen weeks respectively, and finds no significant correlation. Meanwhile, some studies do show some small correlation between successive daily returns. For example, Fama (1965) finds a correlation coefficient of 0.026 for a period of one day. Lo and MacKinlay (1988) and Conrad and Kaul (1988) have performed correlational studies on portfolio stocks. They find that weekly returns of large-cap stock portfolios show almost no correlation, whereas as much as nine percent of the weekly return of a portfolio of smaller stocks can be explained by the return of the previous week. The higher correlation among small-stock portfolios may result from infrequent trading.

Another tool of technical analysis is the filter rule. This class of rules states that, for a given security, the price

fluctuates between two barriers around some "fair" price. When new information comes to the market, however, the fair price and range may shift to a new equilibrium. A shift to a new equilibrium is signaled by a breakout through one of the barriers. Technical analysts claim that, when such a breakout occurs, investors should buy the stock to capitalize on the impending gains or sell the stock to avoid further losses.

Besides the conventional approaches, a number of useful tools were introduced to test the hypothesis, such as the run test and the filter rule. Fama and Blume (1966) have studied a number of possible filter sizes. Although a very small filter can outperform a buy-and-hold strategy over time, transaction costs make such a strategy unprofitable since it requires frequent buying and selling. This is consistent with the small daily correlation. In summary, although technical analysts claim that their techniques can earn abnormal profits, the evidence does not support their presumption of market efficiency.

It is clear that the preponderance of traditional measures support the weak-form market efficiency hypothesis. This is particularly true since transaction costs would eliminate whatever small excess profits can be earned by studying past price movements. Thus, it appears that, given only universally available price and market data, stock prices are indeed unpredictable.

In the last few decades, scientists in the natural sciences have recognized that many processes that were previously thought to be stochastic are actually chaotic (see papers by Domotor & Batitsky, and by Domotor). Even low-dimension nonlinear systems can produce stochastic-like behavior. This suggests that some time-series of economic processes may appear random but are actually chaotic, possibly contaminated by random noise.

The *embedding theorem* provides a procedure for redesigning (embedding) the system's trajectories in phase space from the observation of a single signal. The redesigned phase space portrait is the topological equivalent to the exact one. Since deterministic chaos occurs in a finite-dimension space while random noise does not, this algorithm provides the means to distinguish between the deterministic, but apparently disordered, behavior of a chaotic system and a truly random one. When the data represents a chaotic system, the attractor's dimension will initially increase as the embedding space dimension increases, eventually attaining an asymptotic value. In contrast, when the data represents a truly random system, the attractor's dimension will continue to increase as the embedding space dimension increases.

We mentioned earlier that the Lyapunov exponent indicates the rate of divergence of the trajectories. The existence of a positive Lyapunov exponent is often used as an indication of chaos. A problem in estimating Lyapunov exponents is that

commonly used algorithms require a large number of observations. Since few economic series of such large size are available, Lyapunov exponent estimates of economic data may not be so reliable.

Researchers have applied tools of dynamic system analysis to economic data. A study by Frank, Gencay, and Stengos (1988), demonstrates that the correlation dimension of quarterly GDP data since 1960 for Italy, Japan, the UK, and West Germany increases monotonically as a function of the embedding space dimension less than 15. They have also found that the largest Lyapunov exponents for their data were negative in most cases. Hence, they conclude that there is no evidence of deterministic chaos in their data. Frank and Stengos (1988), too, have computed negative Lyapunov exponents for Canadian macroeconomics series, and have found no evidence of deterministic chaos.

Bajo-Rubio, Fernandez-Rodriguez, and Sosvilla-Rivero (1992) have since examined the Spanish Peseta-Dollar spot and forward exchange rates at various periods. They computed the correlation dimensions as a function of the embedding space dimension (less than 12) as well as the Lyapunov exponent of the series. They observed that the correlation dimension achieves an asymptotic value between 2 and 3 and that the largest Lyapunov exponent is positive. This constitutes evidence of chaotic behavior. Using their model, the authors sought to predict also of the one- and three-month forward rates, but these yielded root mean square

errors lower than those obtained from forecasts from a random-walk model. One may conclude therefore that evidence of chaos in economic data is inconclusive.

Motivated by the study of linear systems, a frequent starting point when analyzing time-series is the construction of the power spectrum, such as the one seen in Figure 2, which is equivalent to the computation of the autocorrelation. The power spectrum may assist in the discovery of periodic or quasi-periodic behavior. Saligari and Snyder (1997) find that, although the model is generally not useful in forecasting the underlying long-run trend, it may be advantageous for short-term predictions of the data. In linear systems, modes in the power spectrum correspond to generalized degrees of freedom of the system, and broad-band power spectra are generated by an infinite-dimensional system. This is not true, however, in nonlinear systems; some low-dimension chaotic systems may well exhibit broad-band power spectra.

In order to determine whether the economy is chaotic or not, once we utilized methods of dynamic systems to analyze the daily returns of nine major stock indices (Shachmurove, Yuen, and Bau, 1999). Our group tried to test the weak-form market efficiency hypothesis in a new way by attempting to find low-order deterministic chaos in stock price data. The data analyzed by us included the stock indices of Canada, Europe-14, Europe excluding the UK, World excluding USA, France, Germany, Japan, the UK, and

the USA, during the period from January 1, 1982, to September 5, 1997. For the purposes of our report, we analyzed the relative daily changes in the stock price indices expressed in percentages. We calculated the percentages from returns converted to U. S. Dollars (Shachmurove, Yuen, and Bau, 1999). The power spectra of the daily returns of stock price indices were depicted as a function of frequency (see Figure 9).

INSERT FIGURE 9

Note that all of the daily returns have a broad-band power spectrum, which implies lack of periodicity in the data. Although this type of power spectrum is consistent with random behavior, it is also common to many chaotic systems; for example, in the logistic map (Gershefeld, 1988).

Figure 10 depicts the probability distribution function as obtained from histograms of the daily returns of the stock price indices. The horizontal axis represents the daily return, and the vertical axis represents the probability of obtaining this return.

Insert Figure 10

The figure indicates that all the daily returns of stock price indices are nearly Gaussian, having a bell-shaped distribution. Although the Gaussian probability distribution is

common in many stochastic processes, it is also exhibited by some chaotic, deterministic systems.

Figure 11 depicts the information dimension, D_I , of the daily returns of the stock price indices, expressed in US dollars, of different exchanges as a function of the embedding dimension, n . Briefly, the embedding space is divided into $N(\epsilon)$ n -dimensional cubes with edge size ϵ . One counts the number of points in each cell, to obtain an estimate of the probability (p_i) of finding a point in cell (i). The information dimension is defined as:

$$\lim_{\epsilon \rightarrow 0} \left(\frac{\sum_{i=1}^{N(\epsilon)} p_i \log(p_i)}{\log(\epsilon)} \right)$$

For a more detailed exposition of the information entropy see Shannon (1948). The largest 11-k value sets are used in the construction of Figure 11. The information dimension obtained using the largest k-sets is generally considered to be less susceptible to noise and therefore more reliable. The vertical bar represents the root mean square (rms) of the oscillations in D_I . Due to the smallness of the rms, the vertical bars are not always visible.

INSERT FIGURE 11

Note that, as (n) increases so do (D_I) and the rms of oscillations in D_I . For example, as n increases from 1 to

the rms of the oscillations in D_I for the Canadian stock price index increases from 0.01 to 0.49. In many cases (Figures 11a, e, and g), D_I approximately equals n , i.e., the curve nearly follows a 45-degree line.

The dimensions of the German (Figure 11f) and USA (Figure 11i) daily returns appear to approach an asymptote at a large value of n . Once larger embedding dimensions are included in the analysis, however, the information dimension of the German and USA indices increases further. Figure 11 as a whole, indicates that the daily returns of all the stocks' price indices are either random or a result of a high-dimension, deterministic process.

Thus, the results indicate that the daily returns are not governed by a low-dimension, deterministic system. However, due to the limited number of data points, the results should be considered as indicative and tentative. In order to have a more reliable estimate for large embedding dimensions a much larger data set would be required. This finding is consistent with the weak-form market efficiency hypothesis. The weak-form market hypothesis states that prices of future securities cannot be predicted from current and/or past price and market information, and thus investors cannot reliably earn abnormal returns merely by examining such publicly available information. Panas and Ninni (2000) have arrived at similar conclusions when analyzing oil futures.

Like physical systems, economic systems represent the aggregate of a vast number of individual, possibly random, actions that allow for statistical generalizations. Elementary particles, however, obey laws of physics that do not change over time. In contrast to physical systems, peoples' choices reflect perceived needs and desires that do change over time. These preferences are influenced by many factors such as new inventions that lead to new options, changing value systems and political structures, and government regulations. Whether one can construct a model that accounts for this added complexity is an open question (see papers by Krippendorff and also by Reiner, Teune and Tomazinis).

Summary

Before the advent of chaos theory, it was believed that complicated, stochastic-like behavior could be generated only by complicated mathematical models with large numbers of degrees of freedom (i.e., models consisting of partial differential equations such as the Navier-Stokes equations or a large number of ordinary differential equations) and/or by stochastic systems. Perhaps one of the most exciting consequences of dynamic system theory is the realization that relatively simple dynamic systems, which can be described by just a few non-linear, ordinary differential or difference equations, can exhibit very complicated, stochastic-like behavior.

This observation gives hope that, in some cases, complicated dynamic behavior can be formulated by low-dimensional mathematical models (i.e., a relatively small number of equations). The possibility of low-dimensional modeling of complicated behavior has tremendous practical applications. Low dimension models allow us to simulate processes inexpensively; they enable us to gain insights into the underlying physical mechanisms, and assist us in identifying important variables in processes; not least, they guide us in devising strategies to control these processes.

One of the hallmarks of chaotic systems is their sensitivity to initial conditions and small perturbations (noise). When one is modeling real systems, the initial conditions are not precisely known and all real systems are subject to perturbations and noise. Hence long term prediction of the detailed behavior of a chaotic system is impossible. The lack of long-term predictability is a fundamental property of chaotic systems just as the uncertainty principle is a cornerstone of quantum mechanics. One of the practical implications is that when one deals with chaotic systems, the availability of large computational resources will not enable one to generate long-term predictions. In the context of meteorology, for example, if the weather system is chaotic (as many believe it to be), long-term weather patterns may well remain unknowable and indeterminable, after all.

References

- Bajo-Rubio, O., F. Fernandez-Rodriguez, and S. Simon-Rivero, (1992) "Chaotic Behaviour in Exchange-Rate Series, First Results for the Peseta-U.S. Dollar Case," *Economics Letters*, 39, pp. 207-211.
- Conrad, J. and G. Kaul, (1988) "Time-Variation in Expected Returns," *Journal of Business*, 61(4), pp. 409-425.
- Cootner, P., (1974) *The Random Character of Stock Market Prices*, Cambridge, MA: MIT Press.
- Dechert, W. and R. Gencay, (1992) "Lyapunov Exponents as a Nonparametric Diagnostic for Stability Analysis," *Journal of Applied Econometrics*, 7, pp. S41-S60.
- Fama, E., (1965) "The Behavior of Stock Market Prices," *Journal of Business*, 38, pp. 34-105.
- Fama, E., (1970) "Efficient Capital Markets: Review of Theory and Empirical Work," *Journal of Finance*, 25, pp. 383-417.
- Fama, E. and M. Blume, (1966) "Filter Rules and Stock Market Trading," *Journal of Business*, 39, pp. 226-241.
- Fama, E. and J. MacBeth, (1973) "Risk, Return, and Equilibrium: Empirical Tests," *Journal of Political Economy*, 81:3, pp. 607-636.
- Forsyth (1994), "Foreword" in Dimitris N. Chorafas, *Chaos Theory in the Financial Markets*, Probus Publishing Company, Chicago, Illinois.
- Frank, M., R. Gencay, and T. Stengos, (1988) "International Chaos," *European Economic Review*, 32, pp. 1569-1584.
- Frank, M. and T. Stengos, (1988) "The Stability of Canadian Macroeconomic Data as Measured by the Largest Lyapunov Exponent," *Economics Letters*, 27, pp. 11-14.
- Gershenfeld, N., (1988) "An Experimentalist's Introduction to the Observation of Dynamical Systems," *World Scientific*, edited by Hao Bai-Lin.
- Gleick, J., (1987) *Chaos*, Viking.

- Lo, A. and C. MacKinlay, (1988), "Stock Market Prices Do Not Follow Random Walks: Evidence from a Simple Specification Test," *Review of Financial Studies*, 1(1), pp. 41-66.
- Lorenz, I (1963) "Deterministic Nonperiodic Flow," *Journal of the Atmospheric Sciences*, 20, pp. 130-141.
- Lorenz, H. W. (1993) *Nonlinear Dynamical Economics and Chaotic Motion*, Springer-Verlag, pp. 201-232.
- Medio, A. (1992) *Chaotic Dynamics*, Cambridge University Press, pp. 101-114.
- Panas, E. and V. Ninni, (2000) "Are Oil Markets Chaotic? A Non-linear Dynamic Analysis," *Energy Economics* 22:5, October, pp. 549-68.
- Peitgen, H., P., and Richter, P., H., (1986) *The Beauty of Fractals*, Springer Verlag.
- Poincaré, H., (1913) *The Foundation of Science: Science and Method*, English translation, 1946, The Science Press, Lancaster, PA, p. 397.
- Saligari, G. R. and R. D. Snyder, (1997) "Trends, Lead Times and Forecasting," *International Journal of Forecasting*, 13:4, December, pp. 477-88.
- Shachmurove, Y., P. K. Yuen, and H. H. Bau, (1999) "Chaotic Systems Analysis of Major Stock Market Indices," *Global Finance International Conference Yearbook*, Istanbul, Turkey, pp. 70-72.
- Shannon, C. E., (1948) "A Mathematical Theory of Communication," *Bell System Technology Journal*, 27, pp. 379-423, 623-656.
- Singer J, Wang Y-Z, and H. H. Bau, (1991) "Controlling a Chaotic System," *Physical Review Letters*, 66, pp. 1123-1126.
- Volterra, V., (1926) "Fluctuations in the abundance of a species considered mathematically," *Nature*, 118, pp. 558-60.
- White, H., (2000) Reality Check for Data Snooping, *Econometrica*, 68:5, 1097-1126.

LIST OF CAPTIONS

1. Schematic description of the Lorenz loop.
2. The flow rate (X) in the loop is depicted as a function of time. The figure depicts two time-series with slightly different initial conditions.
3. The chaotic attractor constructed in three-dimensional phase space.
4. Poincaré section of the chaotic attractor depicted in Figure 3.
5. A schematic description of the magneto-hydrodynamic stirrer. The cavity C contains electrolyte solution. A , B , and C are electrodes. The magnetic field is directed out of the page.
6. The flow field (streamlines) in the cavity when a potential difference is imposed across electrodes A - C .
7. Poincaré sections (stroboscopic images) obtained by following passive tracers when the period is small (left), intermediate (middle), and large (right).
8. The deformation of a material blob at various times $t=kT$. $t=0, 10T, 20T, 30T, 40T$, and $50T$.
9. The power spectra of the daily returns of stock price indices are depicted as functions of frequency. (a): Canada; (b): Europe-14; (c): Europe Excluding the UK; (d): World Excluding USA; (e): France; (f): Germany; (g): Japan; (h): UK; (i): USA.
10. The probability distribution functions of the daily returns of stock price indices are depicted as functions the daily

return. (a): Canada; (b): Europe 14; (c): Europe Excluding the UK; (d): World Excluding USA; (e): France; (f): Germany; (g): Japan; (h): UK; (i): USA.

11. The information dimension, D_I , of the daily returns of stock price indices, expressed in US dollars for each stock exchange (a to i) respectively, is depicted as a function of the embedding dimension, n . The largest 11-k value sets were used in the construction of the figures. The vertical bar represents the root mean squared (rms) of the oscillations in D_I . (a): Canada; (b): Europe-14; (c): Europe Excluding the UK; (d): World Excluding USA; (e): France; (f): Germany; (g): Japan; (h): UK; (i): USA.

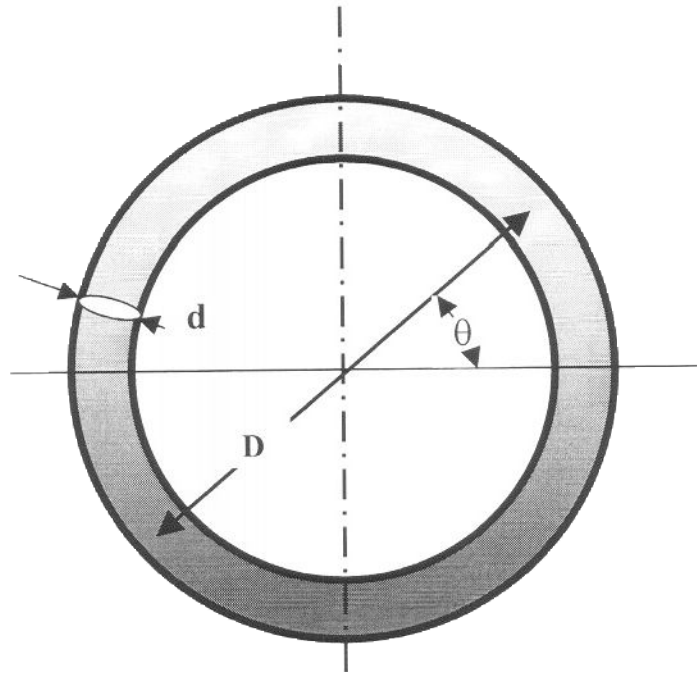


Fig. 1: Schematic description of the experimental apparatus.

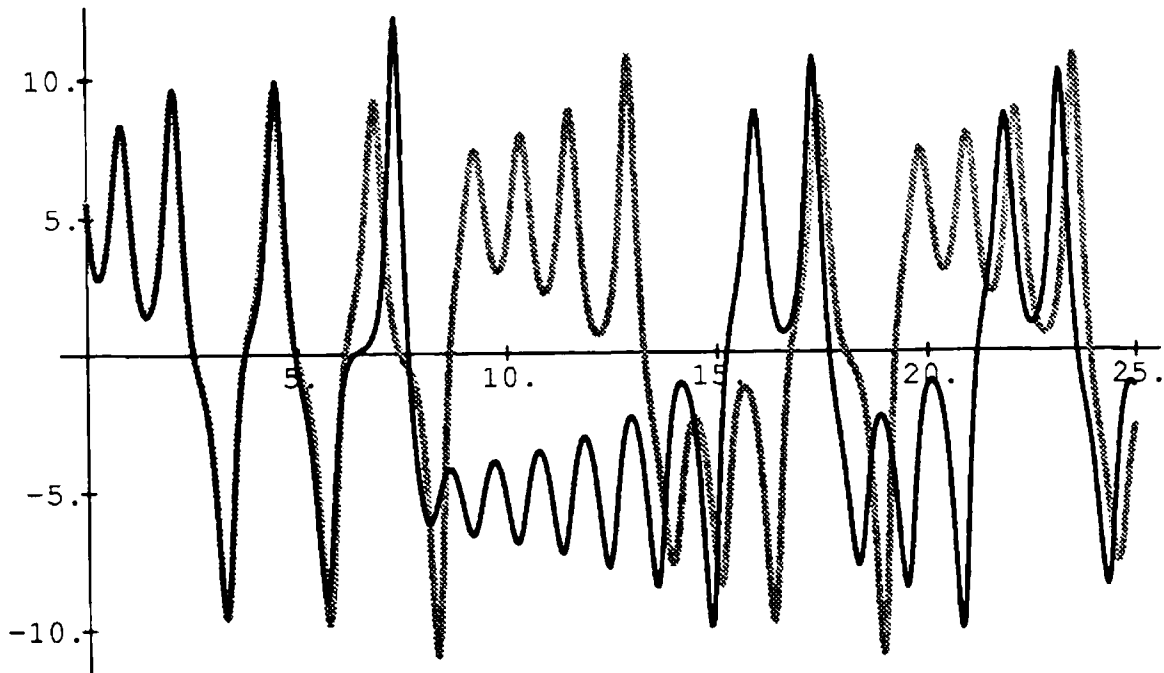


Fig. 2: The flow rate (X) in the loop is depicted as a function of time. The figure depicts two time series resulting from slightly different initial conditions.

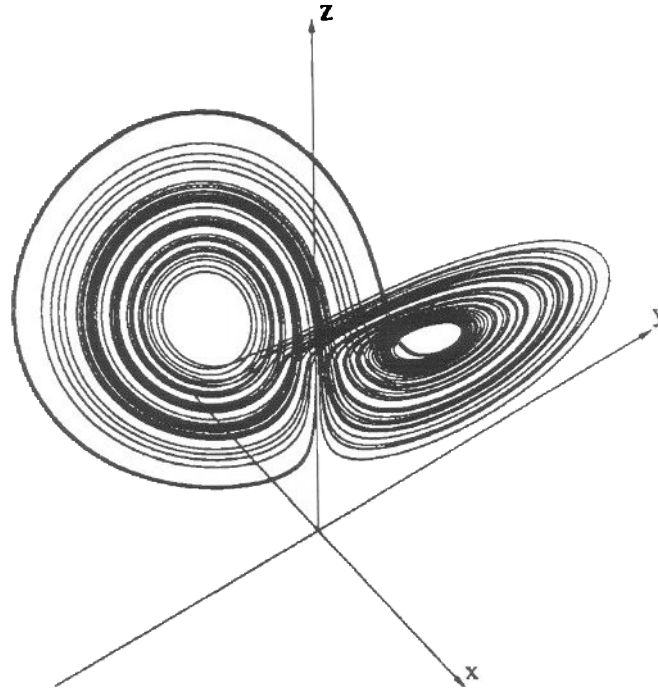


Fig. 3: The chaotic attractor constructed in three-dimensional phase space.

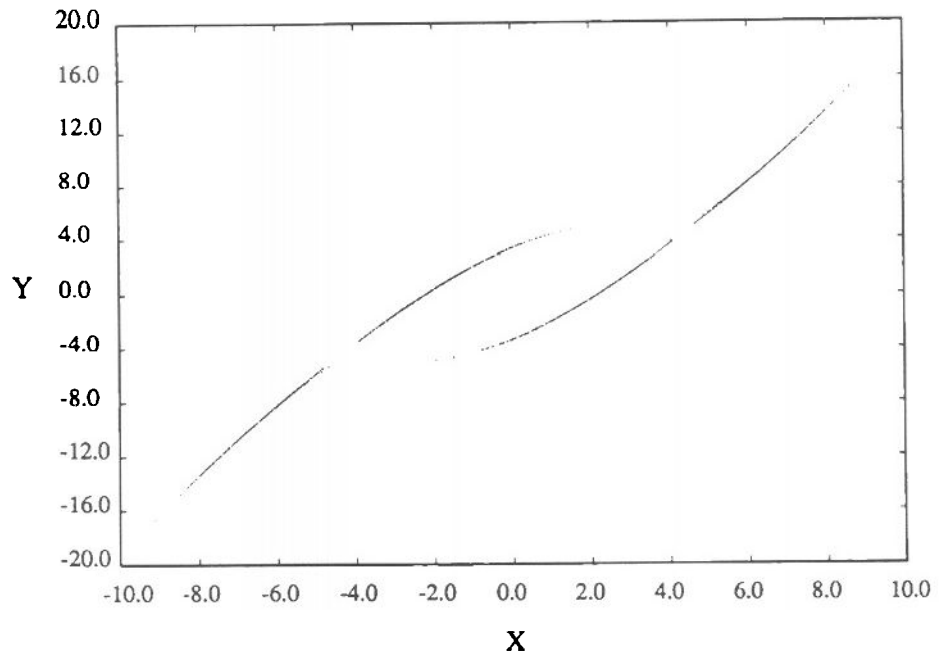


Fig. 4: Poincare section of the chaotic attractor depicted in Fig. 3.

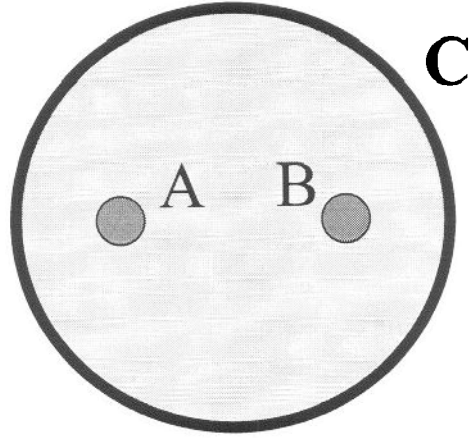


Fig. 5: A schematic description of the magneto hydrodynamic stirrer. The cavity C contains electrolyte solution. A, B, and C are electrodes. The magnetic field is directed out of the page.

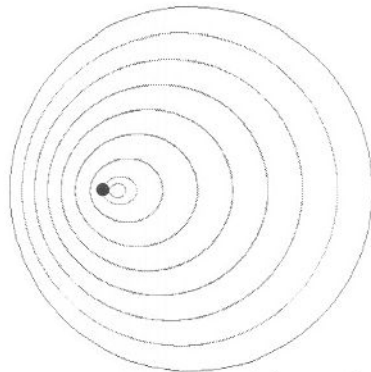


Fig. 6: The flow field (streamlines) in the cavity when a potential difference is imposed across electrodes A-C.

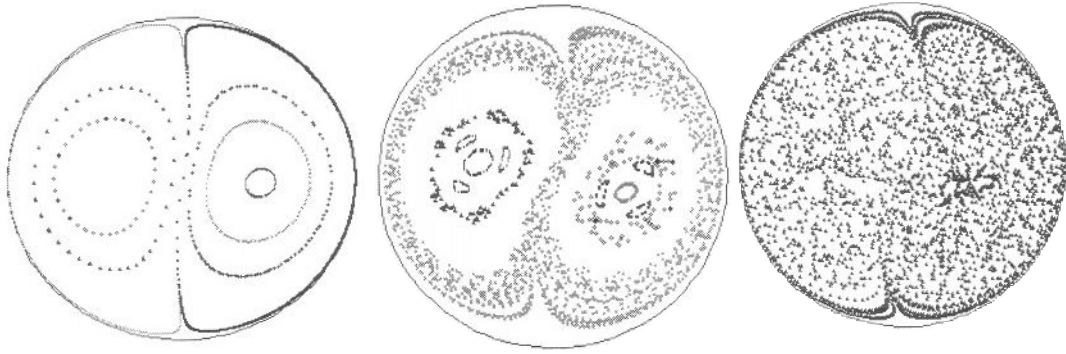


Fig. Poincaré sections (stroboscopic images) obtained by following passive tracers when the period is small (left), intermediate (middle), and large (right)

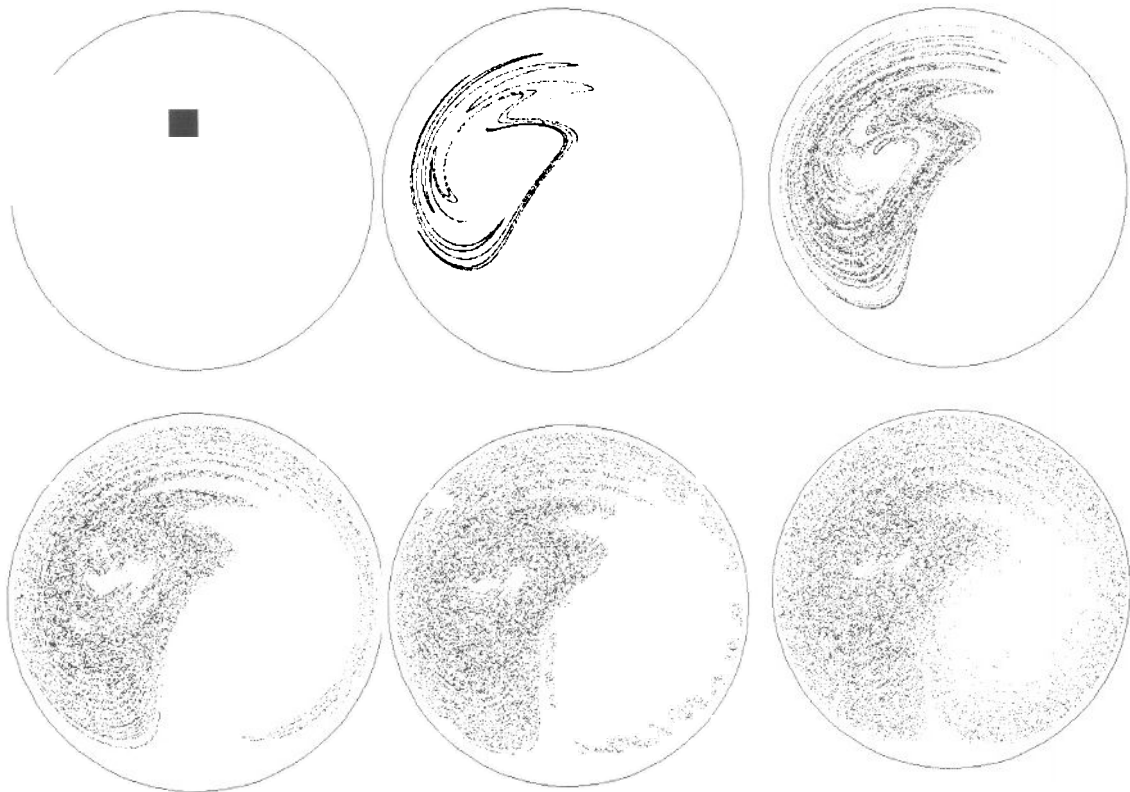


Fig. deformation of material blob at various times $t=kT$.
 $t=0, 10T, 20T, 30T, 40T, 50T$.

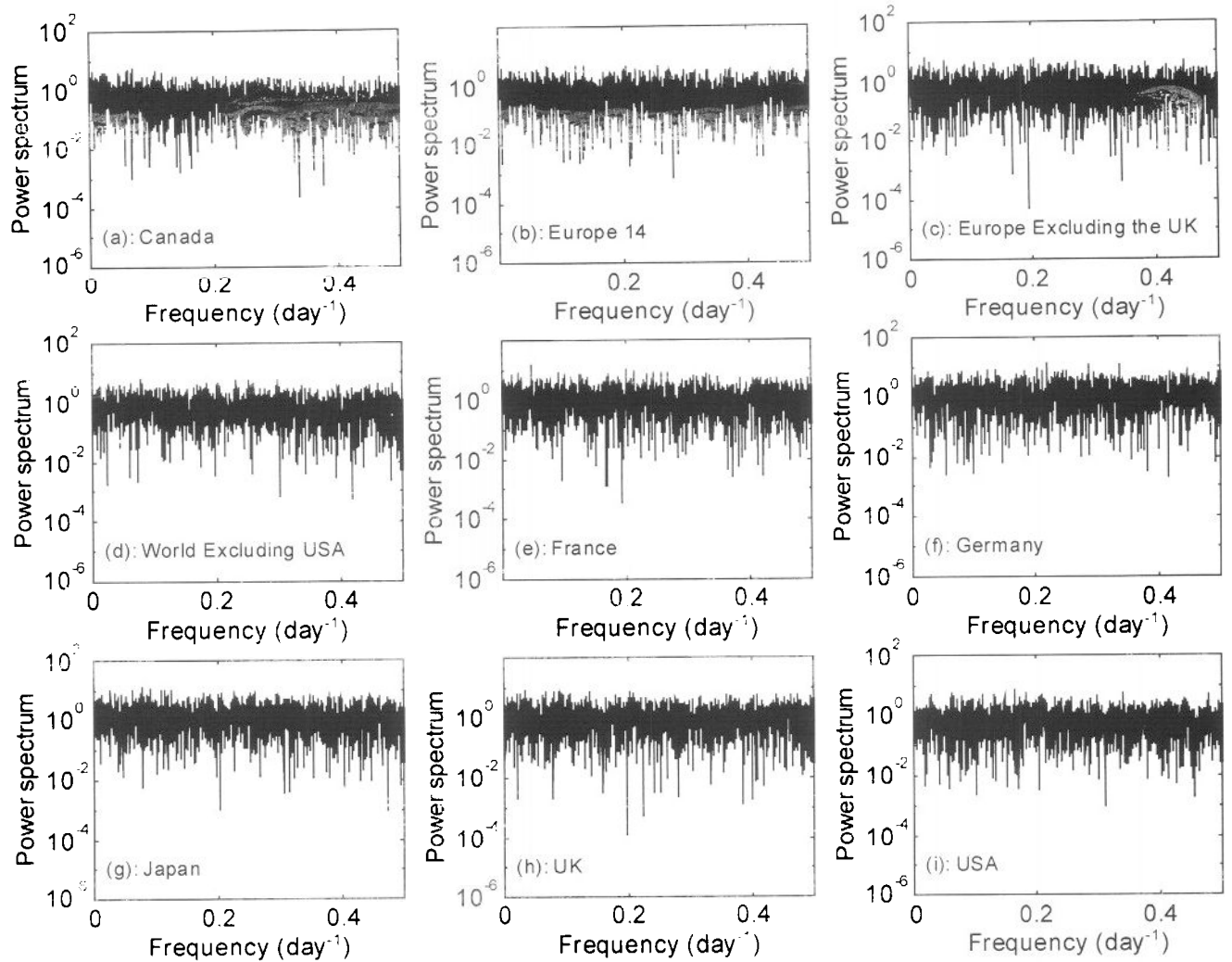


Figure 1 The power spectra of daily returns of stock price indices are depicted as functions of frequency. (a): Canada; (b): Europe; (c): Europe Excluding UK; (d): World Excluding USA; (e): France; (f): Germany; (g): Japan; (h): UK; (i): USA.

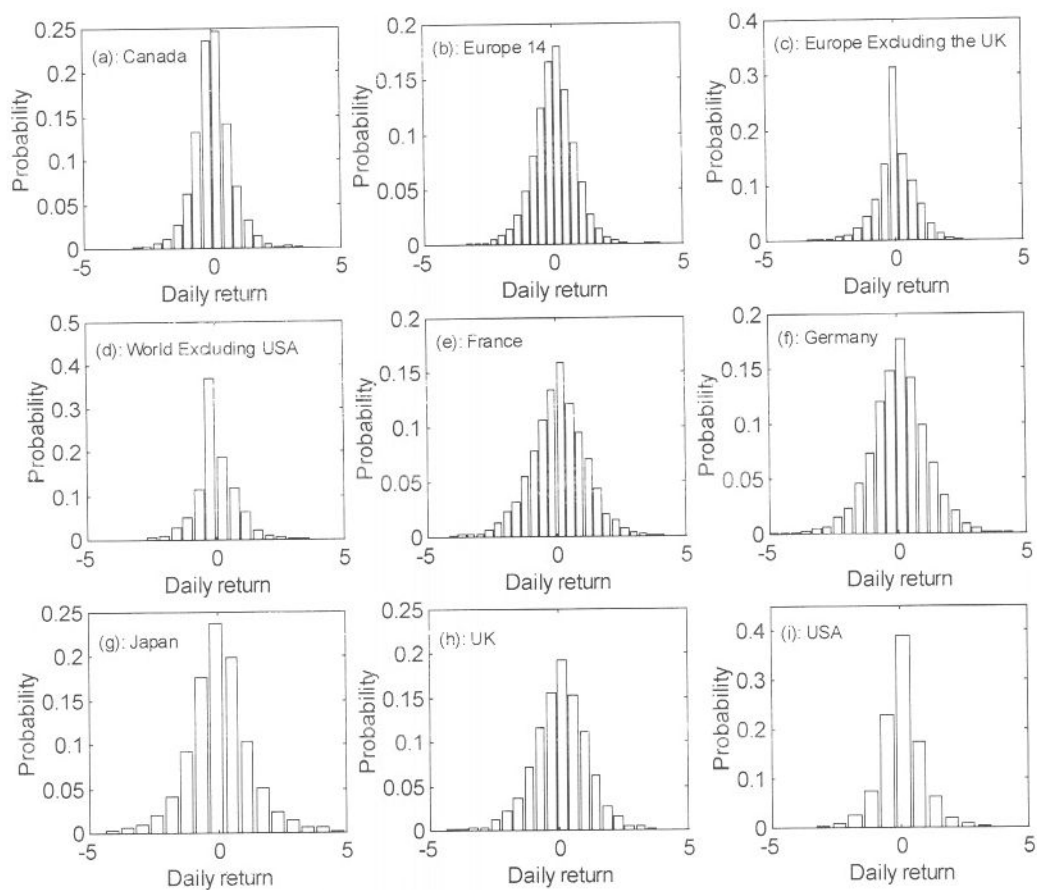


Figure 10. The probability distribution functions of the daily returns of stock price indices are depicted as functions of the daily return. (a): Canada; (b): Europe 14; (c): Europe Excluding the UK; (d): World Excluding USA; (e): France; (f): Germany; (g): Japan; (h): UK; (i): USA.

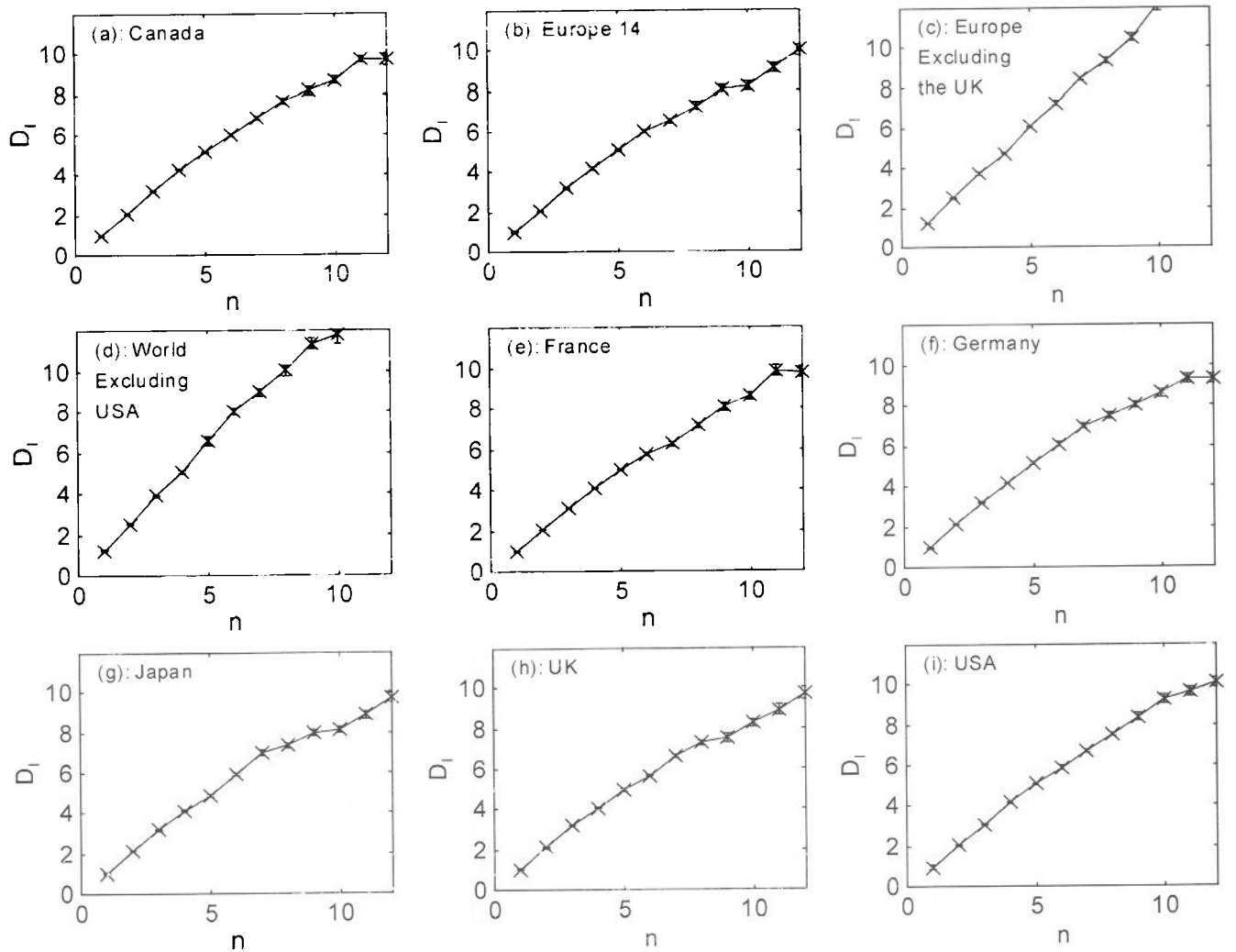


Figure 11. The information dimension, D_1 , of the daily returns of stock price indices, expressed in US dollars, of different exchange is depicted as a function of the embedding dimension, n . The largest 11-k value sets were used in the construction of the figures. The vertical bar represents the rms of the oscillations in D_1 . (a): Canada; (b): Europe 14; (c): Europe Excluding the UK; (d): World Excluding USA; (e): France; (f): Germany; (g): Japan; (h): UK; (i): USA.